Evaluation of Delamination Growth Characterization Methods Under Mode I Fatigue Loading

Gretchen B. Murri

NASA Langley Research Center

Hampton, Virginia

ASC 27th Technical Conference/

15th US-Japan Conference on Composites/

ASTM D30 Meeting

October 1-3, 2012

Arlington, TX

ABSTRACT

Reliable delamination characterization data for laminated composites are needed for input to analytical models of structures to predict delamination. The double-cantilevered beam (DCB) specimen is used with laminated composites to measure fracture toughness, G_{Ic}, delamination onset strain energy release rate, and growth rate data under cyclic loading. In the current study, DCB specimens of IM7/8552 graphite/epoxy supplied by two different manufacturers were tested in static and fatigue to compare the measured characterization data from the two sources, and to evaluate a proposed ASTM standard for generating Paris Law equations. Static results were used to generate compliance calibration constants for the fatigue data, and a delamination resistance curve, G_{IR}, which was used to determine the effects of fiber-bridging on delamination growth. Specimens were tested in fatigue at a cyclic G_{Imax} level equal to 50, 40 or 30% of G_{Ic}, to determine a delamination onset curve and delamination growth rate. The delamination onset curve equations had similar exponents and the same trends. Delamination growth rate was calculated by fitting a Paris Law to the da/dN versus G_{Imax} data. Both a 2-point and a 7-point data reduction method were used and the Paris Law equations were compared. To determine the effects of fiber-bridging, growth rate results were normalized by the delamination resistance curve for each material and compared to the non-normalized results. Paris Law exponents were found to decrease by 31% to 37% due to normalizing the growth data. Normalizing the data also greatly reduced the amount of scatter between the different specimens. Visual data records from the fatigue testing were used to calculate individual compliance calibration constants from the fatigue data for some of the specimens. The resulting da/dN versus G_{Imax} plots showed much improved repeatability between specimens.

Gretchen B. Murri, NASA Langley Research Center, 2 W. Reid St., Hampton, VA 23681, USA

INTRODUCTION

The most common failure mechanism in laminated composite materials is delamination damage. In order to optimize the use of fiber-reinforced composite materials in primary aircraft structures, damage tolerance under static and fatigue loading must be thoroughly understood. Reliable delamination characterization data for laminated composites are needed to use as input in analytical models of structures to predict delamination onset and growth. The double-cantilevered beam (DCB) specimen, shown in Fig. 1, is used to measure mode I fracture toughness, G_{Ic}, and strain energy release rate, G_{Imax}, for delamination onset and growth in laminated composites under mode I fatigue loading. Reference 1 is a standardized test method for measuring static fracture toughness, G_{Ic}, using the DCB specimen. Reference 2 is a standardized test method for determining the onset of delamination and a threshold level, G_{Ith}, below which delamination will not start in fatigue. There is currently no standard for determining the delamination growth rate in fatigue after delamination begins. However, ref. 3 is a proposed test standard for delamination growth in Mode I specimens under constant amplitude fatigue loading and is currently being studied by means of a testing Round Robin through ASTM Committee D30.

For composite materials, delamination growth has typically been related to the cyclic strain energy release rate, G. In refs. 4 and 5, delamination growth onset data from edge-delamination (EDT) and end-notched flexure (ENF) tests were used to generate threshold curves, below which delamination would not initiate. A minimum threshold for no-delamination-growth was assumed to exist at a loading level for which there was no delamination growth at 1 million cycles.

Once delamination begins in a DCB specimen, it typically experiences a region of stable growth. If the delamination growth rate (da/dN) is plotted vs. G_{Imax} on a log-log plot, an equation of the form $da/dN=A(G_{Imax})^B$, called the Paris Law, can be used to characterize this stable delamination growth [4,6].

Because the DCB specimen is unidirectional, some nesting of fibers between adjacent plies can occur, resulting in fiber-bridging at the delaminating interface. As a delamination grows, the fiber-bridging acts to resist the delamination, causing an artificial increase in the measured toughness [5, 7-8], which will affect the resulting Paris Law. However, this fiber-bridging is not a material property, but an artifact of the specimen. In actual structures, delaminations typically grow between

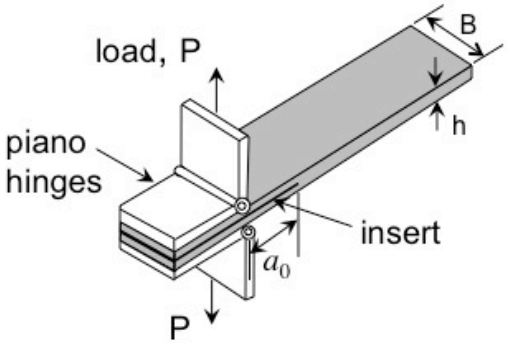

Figure 1. Double-cantilevered beam (DCB) specimen.

plies of dissimilar orientation and fiber-bridging does not occur. Therefore, in order to be useful in structural modeling, expressions relating the delamination growth rate and strain energy release rate must be corrected for the effect of fiber-bridging. Fiber-bridging under quasi-static loading can be quantified as a delamination resistance (G_{IR}) curve, which can be used to correct the growth data for the fiber-bridging effects [9, 10].

In this study, DCB specimens of IM7/8552 graphite/epoxy were tested in static and fatigue to determine delamination characterization properties under Mode I loading. Specimens were provided from two different manufacturers. The IM7/8552 prepreg materials were provided to them and the panels were made according to their own internal specifications, and hence may have slight differences. The objectives of the study were to generate static and fatigue delamination data needed for finite element (FE) modeling of IM7/8552 composite sub-element models, and to compare the static and fatigue results from the two different sources to assess the effect of differences in the same materials due to variations in end-user specifications on characterization data. Similar comparisons were made for the mode II response of IM7/8552 from the same two sources in ref. 11. An additional objective of this study was to evaluate the proposed ASTM standard for generating Paris Law type expressions for delamination growth.

Quasi-static tests were conducted first, to determine the fracture toughness, delamination resistance curve, and test parameters and compliance constants for fatigue loading. Fatigue tests were then conducted at initial G_{Imax} levels of 50, 40, or 30% of G_{Ic}, to determine fatigue delamination onset behavior and growth rates. Both a 2-point and a 7-point secant method were used to reduce the delamination growth data and the resulting Paris Law fits were compared. The delamination resistance equations were used to normalize the growth data to account for the effects of fiber-bridging. A Paris Law fit was applied to both the non-normalized and normalized data sets and the results were compared.

Reference 1 specifies that the modified beam theory (MBT) and modified compliance calibration (MCC) data reduction methods are both acceptable for calculating strain energy release rate, G_I; however MBT is the recommended method because it tends to yield the most conservative values [1]. The specimens used in these tests not only were produced by two different manufacturers, but were also cut from different panels, and consequently had variations in thickness and initial delamination length. Because only the MCC calculation is a function of the specimen thickness, both the MBT and MCC data reduction methods were used to reduce the data, and the results were compared to determine the effect of differences in specimen geometry on calculated G_{Imax}. Also, for some of the specimens, compliance calibration constants were calculated individually from fatigue data and the growth results were compared to results from the static compliance data.

MATERIALS AND SPECIMENS

Specimens of IM7/8552 graphite/epoxy were tested under static and fatigue loading. Specimens were provided from two different suppliers (Source 1 and Source 2), who manufactured the panels and cut them into specimens. The 36-ply,

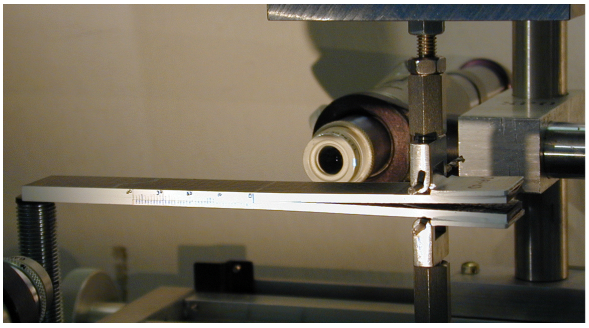

Figure 2. DCB specimen and loading fixture.

0° unidirectional specimens were nominally 1-inch (25.4mm) wide and 7-inch (178mm) long. Prior to testing, specimens were dried using the procedure in ASTM D5229 [12]. All specimens were manufactured with a thin Teflon film at the mid-plane at one end to simulate an initial delamination. The Teflon insert was 0.0005 inch (13μm) thick and nominally 3.0 inch (76.2mm) long.

After drying, the width and thickness of each specimen were measured to the nearest 0.001mm, using a micrometer, at the center and each end. The average specimen width, B, was 0.9989 inch (25.37mm) for Source 1 and 0.9973 inch (25.33mm) for Source 2. The average specimen thickness, h, was 0.176 inch (4.47mm) for both sources. However, specimen thicknesses from different panels varied from 0.1720 inch (4.37mm) to 0.185 inch (4.70mm) for Source 1 and from 0.1681 inch (4.27mm) to 0.192 inch (4.88mm) for Source 2.

Load was applied to the specimens through piano hinges, which were bonded to the specimens using a 2-part epoxy adhesive, which was cured at 300°F for 1 hour. After the specimens cooled, they were stored in a desiccator until testing. A schematic of the DCB specimen is shown in Fig. 1, with the piano hinges, thickness (h), width (B), and initial delamination (a_0) indicated. The initial delamination length is the distance from the load-point line to the end of the insert, and was nominally 2.0 inch (50.8mm). Immediately before testing, the edges of the specimen were coated with a thin layer of white paint and marked in 1mm increments, starting from the tip of the insert to a length of 60mm.

EXPERIMENTAL PROCEDURES

All tests were conducted under displacement control in a small table-top servo-hydraulic test stand using a 100-lb load cell. A photograph of the specimen and test fixture is shown in Fig. 2. The tests were controlled by a computer program, which also recorded the test output data. For all of the static specimens, and approximately half of the fatigue specimens of each source, a 2-Megapixel digital camera was used to monitor the delamination growth and the image was displayed on a computer monitor. Tests were conducted under room temperature conditions. After completing each test, the specimen was split apart at the mid-plane so that the initial delamination length could be more accurately determined, and to verify that the delamination grew evenly across the specimen width.

Static Tests

Quasi-static tests were performed on four specimens from each source to determine the fracture toughness, G_{Ic}. The static tests were also used to determine compliance calibration constants for fatigue data reduction and the delamination resistance curves, G_{IR}. Displacement-controlled static tests were conducted according to ASTM Standard D5528 [1]. Displacement was applied at a rate of 0.02 in/min (0.508 mm/min.) The computer program recorded load, displacement, and compliance every 0.1 seconds. The camera system recorded a photograph of the specimen edge every 0.5 second, along with the corresponding applied displacement and load. The opening displacement rate was applied to the specimen until delamination growth initiated and then was continued until the delamination had grown to at least the 40mm marker. Visual recordings of the delamination length were also made at every 1mm of growth for the first 10 mm, and then at every 5 mm of growth for the remainder of the test.

Fatigue Tests for Delamination Onset Threshold

To generate a delamination onset threshold curve, specimens were tested in fatigue, using the procedures described in ASTM Standard D6115 [2]. Tests were conducted under displacement control, at a frequency of 5 cycles/second. The ratio of minimum displacement to maximum displacement (R-ratio) was $\delta_{min}/\delta_{max}= 0.1$. Prior to fatigue testing, each specimen was loaded quasi-statically, to a maximum displacement that was less than the mean cyclic displacement for that test, in order to determine the initial specimen compliance, and to help verify the location of the insert tip. Specimens of each source were tested at a range of cyclic G_{Imax} levels chosen as a percentage of the average G_{Ic} from the static tests. For each desired G_{Imax} level ($X\%G_{Ic}$), the maximum cyclic displacement (δ_{max}) for testing was determined from the relationship

$$G_{Imax} = X\%G_{Ic} = \frac{3\delta_{max}^2}{2B(a+|\Delta|)} \times \frac{1}{C} \quad (1)$$

where C is the initial specimen compliance, a is the initial delamination length, and $|\Delta|$ is a compliance constant determined from the static testing.

During the fatigue testing, the computer system recorded maximum and minimum loads (P), maximum and minimum displacements (δ), compliance (C), and cycle count (N), at every 10 cycles. The camera system recorded a photograph of the specimen edge at every 1000 cycles, taking the photo at the point of maximum cyclic displacement. A computer file was generated which enabled the photo number to be related to the number of loading cycles at which it occurred.

Fatigue Tests for Delamination Growth Rate

In addition to delamination onset data, fatigue tests were used to generate delamination growth rate data, according to the specifications of the draft standard [3]. The test apparatus, specimen preparation, and procedures required by ref. 3 are

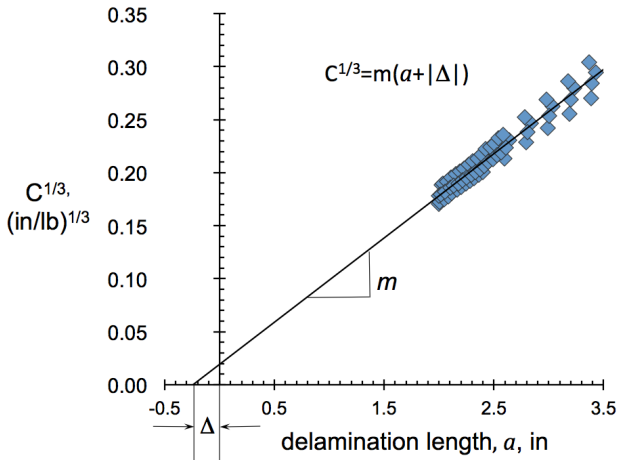

Figure 3. Compliance calibration fit to static data for MBT.

identical to those of standard D6115 (ref. 2) for delamination growth onset. Therefore, each fatigue test specimen was used to generate both delamination onset data and delamination growth data, by cycling to the onset point, and then continuing the fatigue cycling uninterrupted, to generate growth data. Specimens were cycled until the delamination growth rate had decreased to at least $1x10^{-7}$ in/cycle ($2.54x10^{-6}$ mm/cycle), or until no growth had been detected by at least $1.5x10^{6}$ cycles.

RESULTS AND DISCUSSION

Static Tests

COMPLIANCE COEFFICIENTS AND FRACTURE TOUGHNESS

For both specimen sources, fracture toughness was first calculated using the Modified Beam Theory (MBT) method as described in ref. 1, where G_{Ic} is given by

$$G_{Ic} = \frac{3P\delta}{2B(a+|\Delta|)} \tag{2}$$

and where P is the load, δ is the displacement, B is the specimen width, a is the initial delamination length, and $|\Delta|$ is the delamination length correction factor. The relationship between compliance and delamination length for the MBT solution is

$$C^{1/3} = m(a+|\Delta|) \tag{3}$$

The constants m and $|\Delta|$ are determined by a least squares line fit to a plot of the observed delamination lengths (a) from the static test versus the cube root of the corresponding compliance (C). For each source, the combined a vs. $C^{1/3}$ data for all the static specimens were plotted together, as shown in Fig. 3, to determine m and $|\Delta|$ values to use in the data reduction.

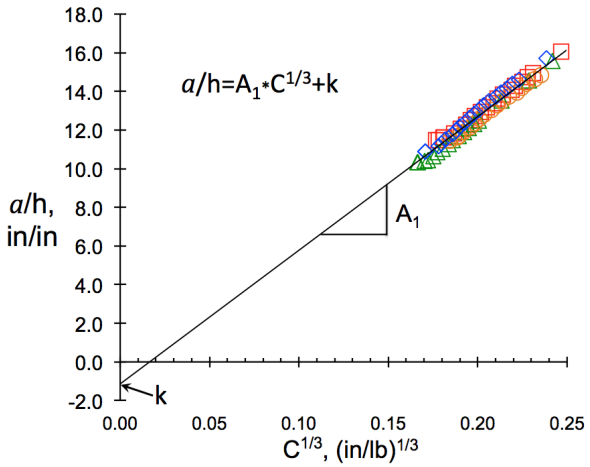

Figure 4. Compliance calibration fit to static data for MCC.

Because of the large thickness variation in specimens cut from different panels, data were also reduced using the Modified Compliance Calibration (MCC) method, for which the compliance relationship is found from a least squares plot of the delamination length normalized by specimen thickness (a/h) versus the cube root of the corresponding compliance:

$$\frac{a}{\mathrm{h}} = \mathrm{A}_1 * \mathrm{C}^{\frac{1}{3}} + \mathrm{k} \tag{4}$$

For each source, the average constants A_1 and k were determined by plotting a/h vs. $C^{1/3}$ data from all the static tests, as shown in Fig. 4. The strain energy release rate for the MCC method is then found from eq. (5) as

$$\mathrm{G_{Ic}} = \frac{3\mathrm{P}^2\mathrm{C}^{2/3}}{2\mathrm{BhA}_1} \tag{5}$$

where P is the failure load, h is the specimen thickness, C is the compliance, and A_1 is the compliance calibration constant determined from the static data.

The compliance calibration coefficients for both the MBT and MCC methods, as well as the static G_{Ic} results for Source 1 and Source 2 are shown in Table I. The

TABLE I. STATIC DCB DATA

	MBT			MCC		
	m, $(in/lb)^{1/3}$/in ($(mm/N)^{1/3}$/mm)	$\|\Delta\|$, in (mm)	G_{Ic}, in-lb/in^2 (J/m^2)	A_1, $(lb/in)^{1/3}$ ($(N/mm)^{1/3}$)	k, in/in (mm/mm)	G_{Ic}, in-lb/in^2 (J/m^2)
Source 1	0.0791 (0.00559)	0.259 (6.57)	1.37 (239.9)	68.8 (38.5)	-1.12	1.37 (239.9)
Source 2	0.0794 (0.00559)	0.243 (6.17)	1.55 (271.4)	69.2 (38.7)	-1.14	1.57 (274.9)

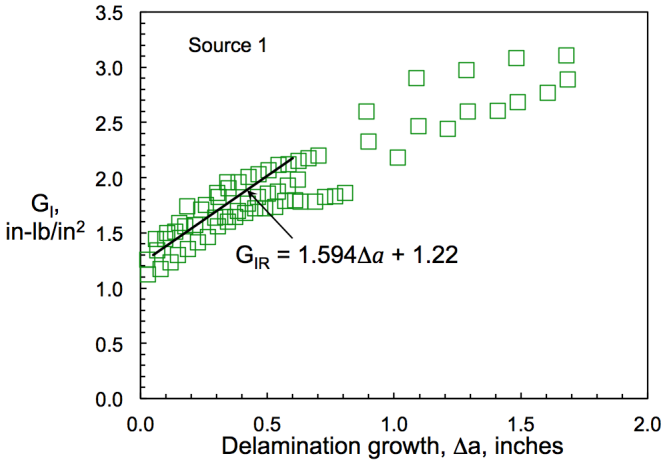

Figure 5. Delamination resistance curve from static DCB tests.

compliance calibration coefficients for both methods were very similar for the two specimen sources. Both the MBT and MCC methods gave an average G_{Ic} value of 1.37 in-lb/in^2 (239.9 J/m^2) for the Source 1 specimens. Average G_{Ic} values for Source 2 were approximately 13% higher than Source 1, at 1.55 in-lb/in^2 (271.4 J/m^2) from MBT and 1.57 in-lb/in^2 (274.9 J/m^2) from MCC. In ref. 11, static end-notched flexure tests were performed on precracked specimens of the same source materials to determine the mode II fracture toughness, G_{IIc}. Measured G_{IIc} values from Source 2 were approximately 9% higher than from Source 1.

DELAMINATION RESISTANCE CURVE

In order to evaluate and correct for the effects of fiber-bridging in the fatigue data, the static test results were also used to determine a delamination resistance curve (R-curve) equation, for each source, to be used in the delamination growth data reduction. During the static testing, after the critical displacement point was reached, opening displacement rate was continued, and G_I was calculated at prescribed increments as the delamination continued to grow. The calculated G-values were plotted vs. the corresponding visually observed increase in delamination length (Δa) to produce an R-curve for each source. Figure 5 shows an example of an R-curve for the Source 1 specimens, where the calculated MCC G-values are shown. The increasing G_I values as the delamination grows indicate that there is some fiber-bridging occurring as delaminations grow in these specimens. As the figure shows, there was an increasing R-curve throughout the loading, with a constant slope for approximately the first 0.5-inch (12.7mm) of delamination growth, followed by another linear region, with a different slope, over the final 1.2 inches (30.5mm) of delamination growth. Because the delamination growth in the test specimens never exceeded 0.5-inch, only the data points at Δa less than 0.5-inch were used to determine the G_{IR} equation. The G_{IR} equation was determined by fitting a least-square curve to the data from each static specimen (Δa <0.5-inch) and averaging the equations. The resulting G_{IR} equation, shown on Fig. 5, was used later to normalize the fatigue growth data. The same method was used to calculate

TABLE 2. DELAMINATION RESISTANCE CURVE (G_{IR}) EQUATIONS

	G_{IR}, MBT method in-lb/in^2	G_{IR}, MCC method in-lb/in^2
Source 1	1.671Δa+1.20	1.594 Δa +1.22
Source 2	1.447 Δa +1.436	1.337 Δa +1.429

a G_{IR} equation for the Source 1 specimens using the MBT results, and for the Source 2 specimens, using both data reduction methods. The resulting G_{IR} equations for both sources from the MBT and MCC methods are shown in Table 2.

Fatigue Tests for Delamination Onset Threshold

To produce a delamination threshold curve, specimens were tested in fatigue at target G_{Imax} levels equal to 50, 40, and 30% of the average G_{Ic} from the static tests. Under displacement control in fatigue, G_{Imax} decreases from the initial value as the delamination grows. Therefore, the applied G_{Imax} listed for each test is the initial value. After the fatigue testing was completed on each specimen, the specimen was split along the midplane, and the initial delamination length was more accurately measured and the initial G_{Imax} was recalculated. Therefore, the actual initial G_{Imax} levels varied from 60% to 27%. A minimum of four specimens from each source was tested at target levels of 50, 40 and 30% G_{Ic}. Additionally, two specimens from Source 1 were tested at target levels over 50%G_{Ic}. To determine the threshold curve, the number of cycles corresponding to a decrease in the specimen compliance of 5% was recorded, as recommended in ref. 2.

Figure 6a shows the onset data and curves for both sources. The average fracture toughness for each source, G_{Ic}, is plotted at N=1. The right-pointing arrows on the data points at the highest N values indicate that these are run-out tests, for which no delamination growth occurred. Results are generally in good agreement for tests at G_{Imax} of 50%G_{Ic} or lower. For Source 2, the results are in reasonably good agreement for most of the data, however, there is noticeably more scatter in the results at the lowest load level. Although there is some overlap between the two

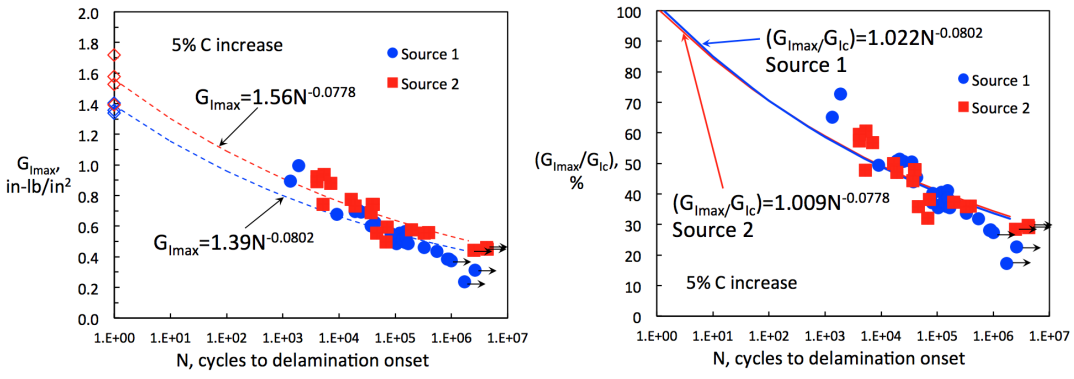

(a) Onset life versus initial G_{Imax}.

(b) Onset life versus %G_{Ic}.

Figure 6. Delamination onset curves for Sources 1 and 2.

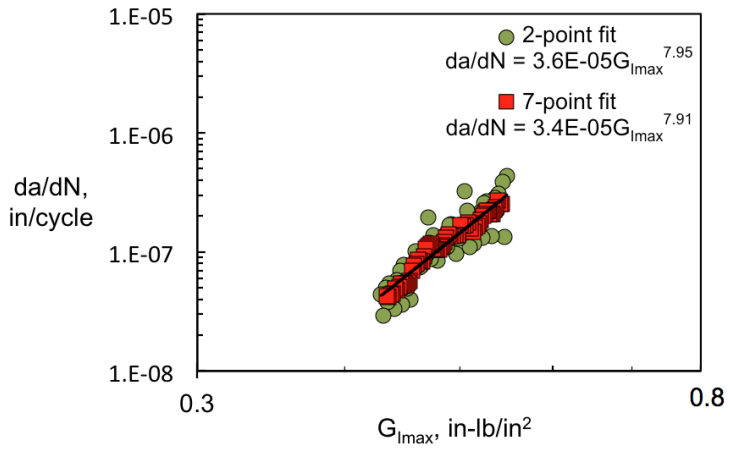

Figure 7. 2-point and 7-point data reduction comparison.

source data sets, the number of cycles to onset is typically higher for the Source 2 specimens compared to Source 1, at comparable G_{Imax} values.

Typically, a power curve is fit through the data sets, to give a G_{Imax} threshold curve below which delamination should not occur [4, 5]. The Kaleidagraph data plotting software [13] was used to find the best-fit power curve for both data sets (excluding the run-out results.) The dashed blue line in Fig. 6a shows the curve fit to the Source 1 data. The dashed red line shows the curve fit to the Source 2 data. The equations are shown on the figure. Although the onset curves have similar exponents and the same trend, at low G_{Imax} levels, the onset life of the Source 2 specimens is almost an order of magnitude greater than Source 1. Figure 6b shows the same data, with the G_{Imax} data expressed as the percentage of G_{Ic} for each material. The onset curves are now almost identical and the equations in terms of G_{Imax}/G_{Ic} are shown on the plot. In ref. 11, delamination onset curves were generated under mode II loading, using specimens from the same sources used in this study. Those curves were found to be nearly identical for the two sources.

Fatigue Tests for Delamination Growth Rate

2-POINT AND 7-POINT d*a*/dN CALCULATION

Reference 3 recommends two methods for determining the delamination growth rate, d*a*/dN, a 2-point method and a 7-point secant method. For the 2-point method, d*a*/dN is determined from the slope of the line between two adjacent points on the plot of *a* (delamination length) vs. N (cycle count.) The corresponding value of G_{Imax} is calculated from either eq. (2) or (5), (MBT and MCC, respectively), where *a*, P, and C are the averaged values from the two data points. The 7-point secant method calculates d*a*/dN by fitting a second-order polynomial to each set of 7 successive data points. The polynomial is used to calculate the value of *a* at the midpoint of the 7-point data set. The corresponding G_{Imax} value is calculated from either eq. (2) or (5), where P and C are the average values over the interval. A complete description of this method can be found in ASTM Standard E647-00 [14].

Figure 7 shows the da/dN vs. G_{Imax} results from both the 2-point and 7-point da/dN calculation methods for a Source 2 specimen tested at 40%G_{Ic}, along with the Paris Law equations fit to each data set. The Paris Law expressions are very similar for the two methods, but the scatter in the data is much less for the 7-point fit method. These results were typical for all the specimens tested, with the exponent of the Paris Law differing by about 3% or less between the 2-point and 7-point methods. Therefore, the 7-point fit method was considered to accurately represent the delamination growth, with less scatter, and was used to represent da/dN for all the tests.

MBT AND MCC DATA REDUCTION

Plots of da/dN vs. G_{Imax} were generated for all the fatigue specimens from both sources, using both the MBT and MCC data reduction methods. Figures 8 and 9 show results for 23 specimens from Source 1, tested at G_{Imax} levels between 73%

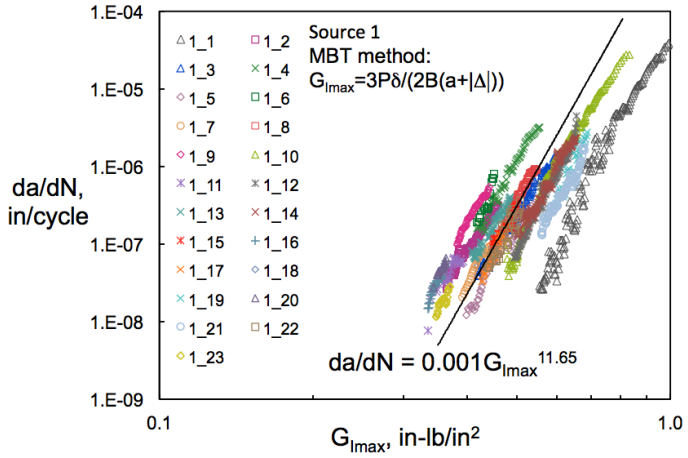

Figure 8. Delamination growth results for Source 1 using MBT.

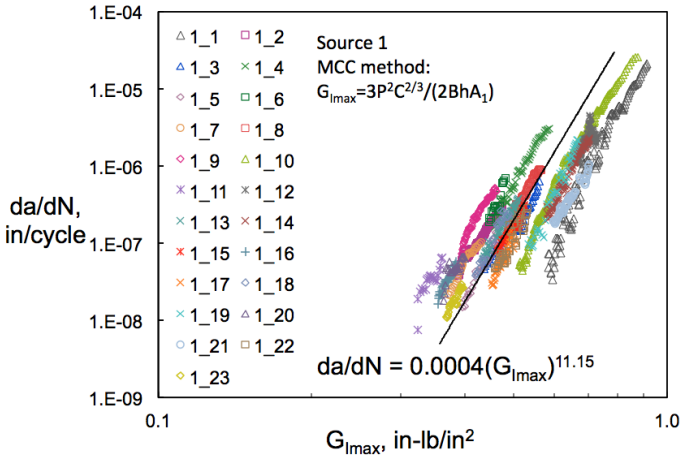

Figure 9. Delamination growth results for Source 1 using MCC.

and 27% G_{Ic}. The results are similar for the two G_{Imax} calculation methods. For both calculation methods, the slopes from the different specimens appear similar, but the position along G_{Imax} varies significantly, with a tendency for the data to shift to the left as the initial G_{Imax} value of the specimen decreases. Figures 10 and 11 show the da/dN vs. G_{Imax} results for 16 Source 2 specimens (MBT and MCC results, respectively.) Again, the data from the two methods are similar, although the MCC results are in a slightly more compact group. Like the Source 1 data, the Source 2 specimens seemed to have similar slopes, but different positions along G_{Imax}, although the data are less spread out than the Source 1 results. The scatter observed in figs. 8-11 is likely due to differences in specimen geometry and varying amounts of fiber-bridging that occurred.

For both sources, using the MCC data reduction caused some specimens to noticeably shift position either to the right or left compared to the MBT solution. This occurred in specimens that were significantly thicker or thinner than the

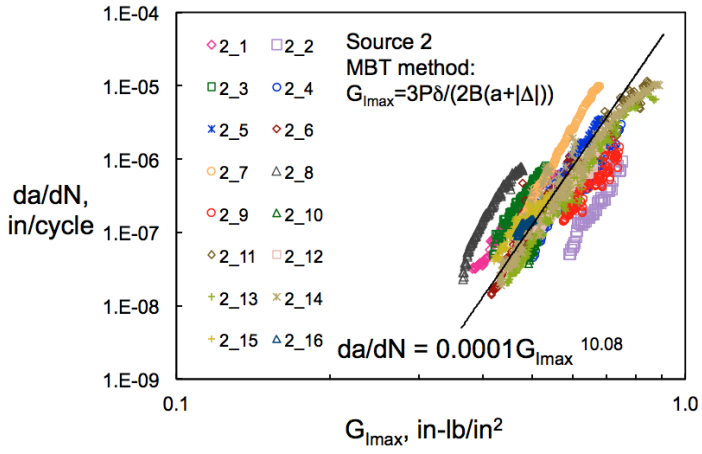

Figure 10. Delamination growth results for Source 2 using MBT.

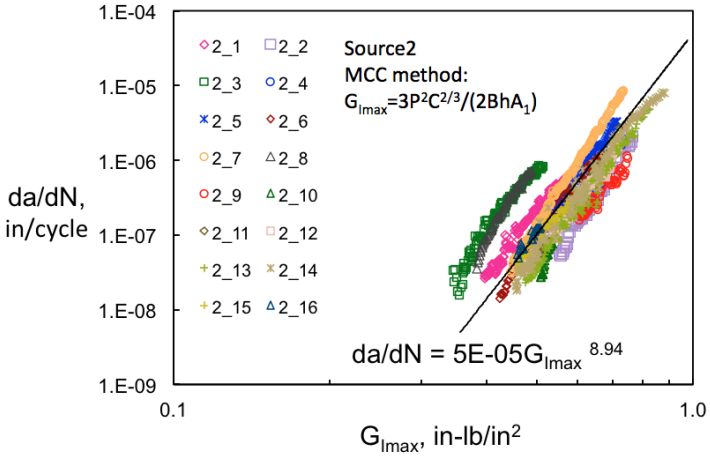

Figure 11. Delamination growth results for Source 2 using MCC.

average. The MCC solution, unlike the MBT, is a function of the specimen thickness, which varied by as much as 8.5% from the average value for some specimens. Specimens with thickness close to the average value showed little difference in the G_{Imax} results for the two data reduction methods.

Because of the range of the data sets across G_{Imax}, fitting a Paris Law equation to the combined data resulted in a line that has a much flatter slope than any of the individual specimens and therefore did not reflect the behavior of the specimens. Therefore, a Paris Law was fit to each specimen and the constants and slopes were averaged for each data set. The resulting equations for each method are shown on the figures. The Paris Law exponents are similar for all the plots, and are slightly lower using the MCC calculation for both sources. However, the constants, which reflect the position along the G_{Imax} axis, are very different, ranging from 0.001 for the Source 1 MBT results, to 0.00005 for the Source 2 MCC results. This value affects the prediction of the delamination growth rate at the onset and at delamination arrest. Because of the spread of the data sets, these values are not very useful for generating a valid Paris Law. Because the MCC and MBT results are similar, and because the MCC results showed less scatter for both sources, only the MCC data reduction results are considered in the remaining discussion.

NORMALIZED G_{IMAX} RESULTS

Because the static specimens exhibited a rising R-curve, it is reasonable to assume that the fatigue data are also affected by fiber-bridging. Therefore, the G_{Imax} data were normalized by the delamination resistance curves and the data were replotted. At each data point, the G_{Imax} value was divided by G_{IR}, using the appropriate equation from Table II. In order to directly compare the unitless normalized results (G_{Imax}/G_{IR}) to the G_{Imax} results, the normalized results were multiplied by G_{Ic}. This value was called $\overline{G_{Imax}}$ and is plotted in fig. 12 along with the non-normalized results for a Source 2 specimen, tested at G_{Imax}=59%G_{Ic}.

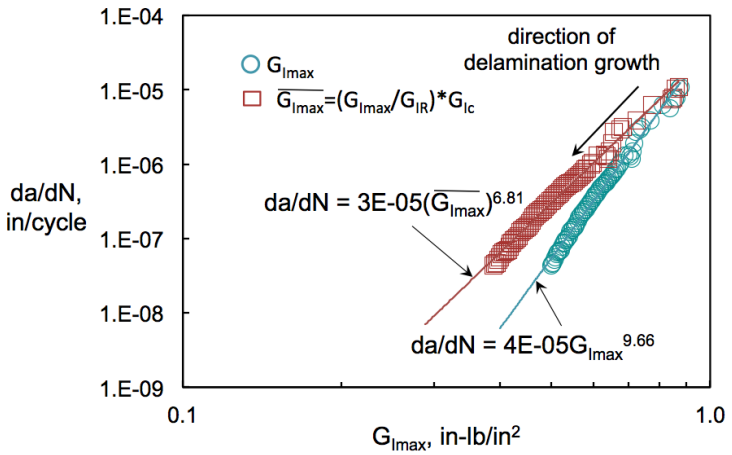

Figure 12. Effect of fiber-bridging correction on Paris Law for Source 2 specimen tested at 59%G_{Ic}.

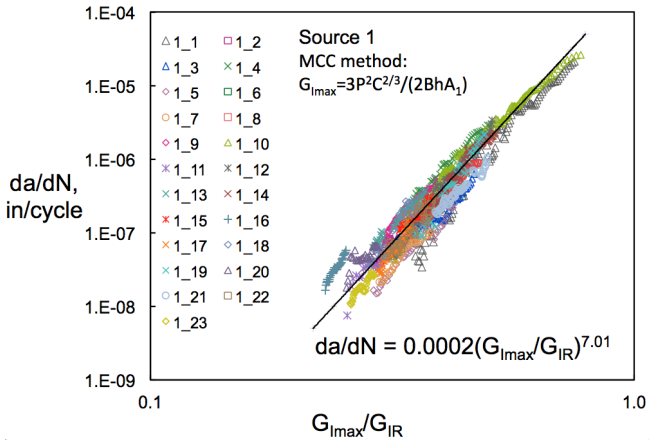

Figure 13. Normalized delamination growth results for Source 1 using MCC.

A Paris Law equation has been fit to each data set. As the figure shows, the slope of the normalized results is not as steep and the exponent of the Paris Law is decreased by 29.5% from the non-normalized results. For all specimens tested, normalizing the G_{Imax} values resulted in a decrease in the Paris Law exponent of between 28.1% and 41.5%, compared to the non-normalized results. The average decrease was 37.1% for the Source 1 specimens and 31.5% for the Source 2 specimens. As Fig. 12 demonstrates, the effect of fiber-bridging on delamination growth rate can be significant, especially at high G_{Imax} levels. For example, when G_I has decreased to 0.5 in-lb/in^2, the normalized results in Fig. 12 show the delamination growth rate to be over 5 times faster than the non-normalized results predict. These results are consistent with the behavior observed in ref. 10, where it was shown that for a material with extensive fiber-bridging, the difference between the normalized and non-normalized delamination rate could quickly become an order of magnitude or more. In a structure where delamination is the dominant failure mode, the effect of fiber-bridging on the mode I delamination growth rate must be recognized as an artifact of the DCB test on a unidirectional layup and the normalized data should be used.

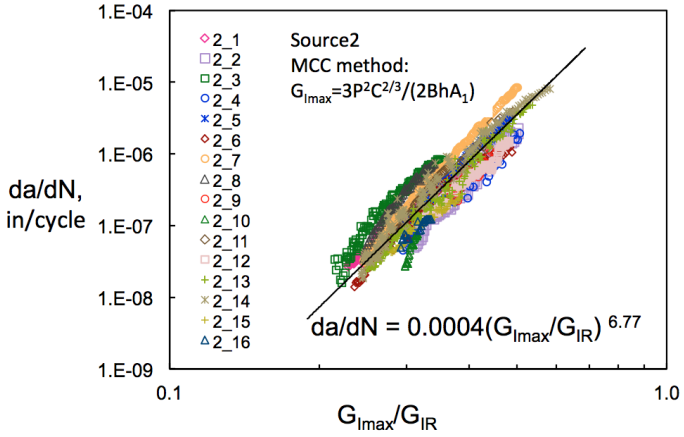

Figure 14. Normalized delamination growth results for Source 2 using MCC.

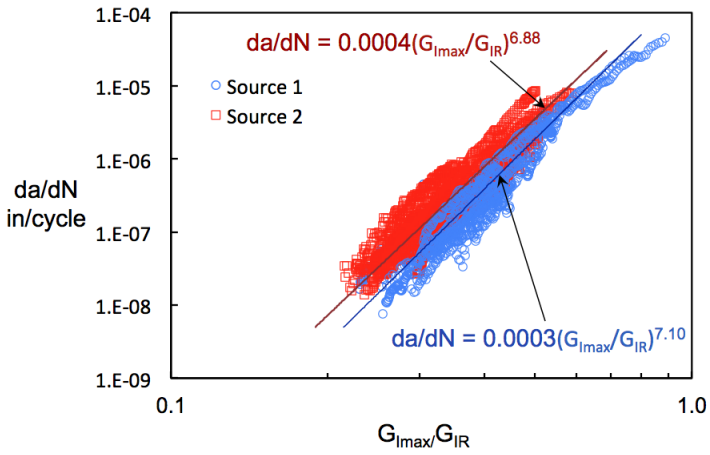

Figure 15. Normalized delamination growth results for Sources 1 and 2.

Figure 13 shows the normalized versions of the data shown in Fig. 9 for Source 1. Comparing Fig. 13 with Fig. 9 shows the effect of normalizing, with the slopes decreasing, and a much more compact data set. The Paris Law expression for Source 1 is shown on the figure.

Figure 14 shows the normalized versions of Fig. 11 for the Source 2 specimens. As for the Source 1 specimens, the slope of the Paris Law and the range of the data are decreased in the normalized data sets. The Paris Law expression is similar to the results for Source 1.

Figure 15 shows the MCC G_{Imax}/G_{IR} data from both sources plotted together. The slopes are similar for the two sources, but the Paris Law constants are different enough that the two data sets do not completely overlap each other due to variations in G_{Ic} and G_{Imax} vs. N. These results are similar to those of ref. 11, where Paris Law expressions were generated for the mode II fatigue growth. Those Paris Laws also had similar exponents for Sources 1 and 2, but different constants, causing the Source 1 and Source 2 data sets to be offset slightly.

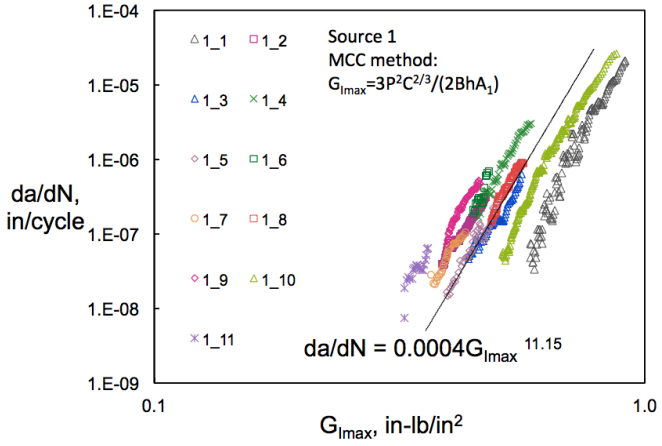

Figure 16. Delamination growth results for Source 1 using compliance calibration constants from static data.

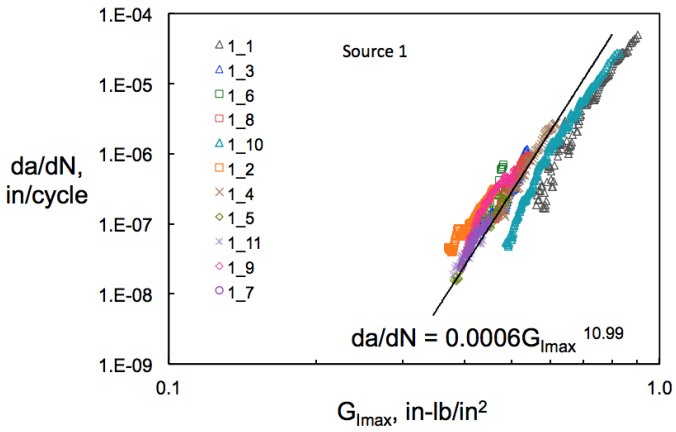

Figure 17. Delamination growth results for Source 1 using individually fit compliance calibration constants from fatigue data.

INDIVIDUAL COMPLIANCE CALIBRATION FIT

The reliability of the fatigue results shown in Figs. 8-15 depends on the accuracy of the compliance calibration constants from the static tests. The compliance calibration constants in Table I were determined by a least squares fit to the combined static data, as shown in Figs. 3 and 4. When the constants are determined from each static specimen separately, the resulting slopes (A_1 and m) are similar to the combined value, differing by less than +/- 5%. However, the intercept values (k and $|\Delta|$) can have significant differences. For the combined Source 1 static specimens, the value of k was -1.12, but for the individual specimens, k varied from -1.09 to -1.79. For the combined Source 2 static specimens, the combined k value was -1.14, but values for the individual specimens ranged from -0.72 to -2.21. To attempt to determine the influence of using averaged static data on the resulting fatigue data and Paris Law, compliance calibration constants based on fatigue results were determined individually for some of the test specimens.

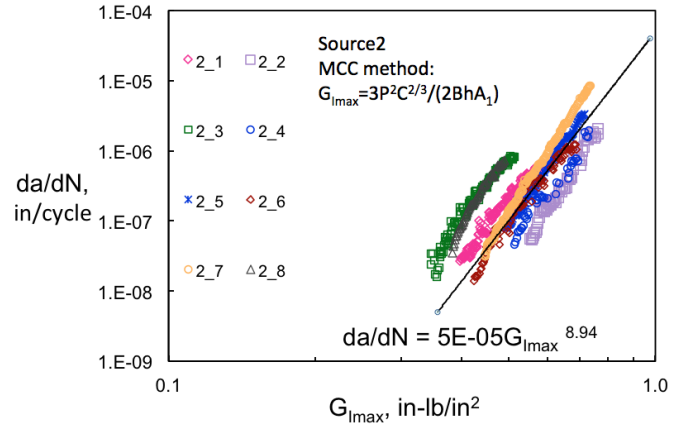

Figure 18. Delamination growth results for Source 2 using compliance calibration constants from static data.

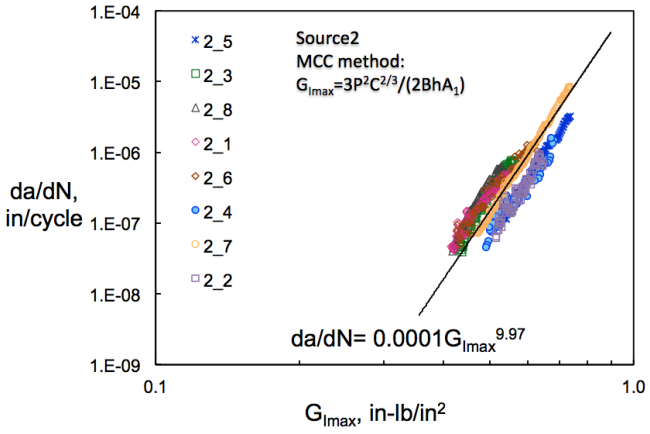

Figure 19. Delamination growth results for Source 2 using individually fit compliance calibration constants from fatigue data.

For every specimen for which there were adequate edge photos or visual recordings of the edge delamination length from the fatigue testing (approximately half of the specimens from each source), the visual data were used to generate a plot similar to Fig. 4. The compliance value corresponding to each observed delamination length was found from the raw fatigue data using the log that related the number of loading cycles to the photo number. A minimum of 4 visual recordings was used for each specimen data fit, with the final recording usually taken at over 800K cycles. The individually fit values of A_1 ranged from 61.0 to 76.8 for the Source 1 specimens and had an average value of 70.1, compared to the combined value of 68.8 from Table 1. The k values ranged from -0.01 to -2.49 with an average value of -1.22. For the Source 2 specimens, A_1 ranged from 63.6 to 76.9 and had an average value of 70.0, compared to the combined value of 69.2. The k values for the Source 2 specimens ranged from -0.05 to -2.63 with an average value of -1.06. After determining A_1 and k for each specimen, the da/dN vs. G_{Imax}/G_{IR} plots were recalculated.

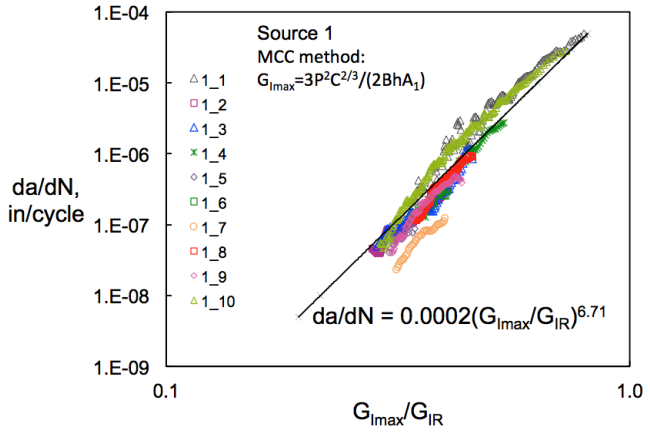

Figure 20. Normalized delamination growth results for Source 1 using individually fit compliance calibration constants from fatigue data.

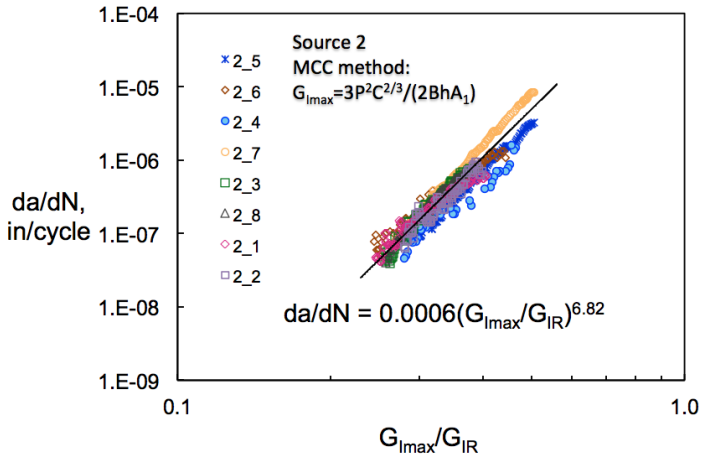

Figure 21. Normalized delamination growth results for Source 2 using individually fit compliance calibration constants from fatigue data.

Figure 16 shows the G_{Imax} results from Fig. 9 (using averaged static compliance parameters) for all the Source 1 specimens for which A_1 and k could be fit. Figure 17 shows the same results calculated using individually fit parameters. The correlation between the specimens is much improved over Fig. 16. The corresponding data for Source 2 are shown in Figs. 18 and 19. Again, using the individually fitted compliance constants resulted in much better alignment of the different specimens. Figures 20 and 21 show the normalized results from Figs. 17 and 19. Both data sets now show very good alignment of the individual specimens. The Paris Law expressions are shown on the plots and are in good agreement. A comparison with the equations on Figs. 13 and 14 shows that the Paris Law parameters did not change significantly.

SUMMARY

Double-cantilevered beam specimens of IM7/8552 manufactured by two sources were tested in static and fatigue to determine delamination characterization data for use in finite element modeling, and to compare the experimental results from the two different sources. Additionally, the fatigue tests were used to evaluate a proposed ASTM standard for determining Paris Law expressions for delamination growth under mode I loading. Data were reduced using both the Modified Beam Theory (MBT) method and the Modified Compliance Calibration (MCC) method.

Static tests were conducted according to ASTM Standard D5528. The static tests were used to calculate fracture toughness, compliance calibration constants and delamination resistance curves for use in the fatigue data reduction.

Fatigue DCB tests were conducted at initial G_{Imax} levels nominally equal to 50, 40 and 30% G_{Ic}, to generate a delamination onset threshold curve, and delamination growth data. Delamination onset curves were generated by plotting the initial G_{Imax} value versus the number of loading cycles to a 5% increase in compliance. Power law expressions were fit to the data plots.

To generate delamination growth data, each fatigue specimen was cycled until the delamination growth rate had decreased to at least $1x10^{-7}$ in/cycle, or until no delamination growth could be detected by at least $1.5x10^{6}$ cycles. The fatigue data were reduced according to the specifications of a proposed draft standard for delamination propagation. Both a 2-point and a 7-point secant method were used to calculate the delamination growth rate, da/dN, for each fatigue specimen. G_{Imax} was calculated using the MBT and MCC data reduction methods. In order to determine the effect of fiber-bridging on the da/dN results, the G_{Imax} values were normalized by the delamination resistance curves, G_{IR}, and replotted versus da/dN. Paris Law equations were fit to the normalized data sets for each source. Compliance calibration parameters were individually calculated for approximately half of the test specimens, using visual data recordings or photos taken during fatigue testing, and the G_{Imax} data were recalculated and compared to the results using averaged static parameters.

The following observations were made:

1. The compliance calibration constants and the delamination resistance curves were very similar for the two sources and for the two data reduction methods. The G_{Ic} calculations from MBT and MCC were identical for each source, however, the Source 2 average fracture toughness was found to be approximately 13% higher than the Source 1 value.
2. The onset threshold curves (G_{Imax} versus N) for Sources 1 and 2 were similar; however, Source 2 specimens had longer lifetimes to delamination onset at every load level, compared to the Source 1 results. When fatigue life was plotted versus the percentage of G_{Ic} for each test, the onset curves were identical for Sources 1 and 2.
3. The 7-point secant data reduction resulted in plots with reduced scatter compared to the 2-point method. The slopes of the Paris Law usually differed by 3% or less. Therefore, the 7-point secant method was considered accurate for calculating da/dN versus G_{Imax} data.
4. For each source, the slopes of the da/dN versus G_{Imax} plots were similar for the specimens tested, but the data sets were spread over a wide range of G_{Imax}. Results from the MCC method tended to be slightly more compact than from MBT, but neither method yielded a plot that was suitable for fitting a Paris Law to the combined data.
5. For both the Source 1 and Source 2 specimens, normalizing the G_{Imax} data by the G_{IR} curve to account for the significant effect of fiber-bridging in these laminates resulted in a decrease in the Paris Law exponent of approximately 31 to 37%. Additionally, the normalized results reduced the spread of the results over G_{Imax} and resulted in a more compact data set.
6. Paris Law equations fit to the normalized data sets for Sources 1 and 2 were almost identical. Additionally, the normalized results reduced the spread of the results over G_{Imax} and resulted in a more compact data set.
7. Fatigue results for the Source 1 and Source 2 materials were reasonably similar for all the computations. The MCC data reduction method gave more consistent results than the MBT method and should be used if there is significant variation in specimen thickness.

8. Using individually fit compliance parameters based on fatigue data resulted in much better agreement between specimens at all G_{Imax} levels than results achieved using averaged parameters from the static results. The normalized G_I results showed excellent alignment of the specimens for both sources.

REFERENCES

1. "ASTM D 5528-01, Standard Test Method for Mode I Interlaminar Fracture Toughness of Unidirectional Fiber-Reinforced Polymer Matrix Composites," in *Annual Book of ASTM Standards*. Vol. 15.03, American Society for Testing and Materials, 2008.
2. "ASTM D 6115-97, Standard Test Method for Mode I Fatigue Delamination Growth Onset of Unidirectional Fiber-Reinforced Polymer Matrix Composites," in *Annual Book of ASTM Standards*. Vol. 15.03, American Society for Testing and Materials, 2008.
3. "Standard Test Method for Mode I Fatigue Delamination Propagation of Unidirectional Fiber-Reinforced Polymer Matrix Composites," Draft standard, ASTM International, Committee D30 on Composites, 2009.
4. O'Brien, T. K., "Towards a Damage Tolerance Philosophy for Composite Materials and Structures," *Composite Materials: Testing and Design (Ninth Volume), ASTM STP 1059*, S. P. Garbo, Ed., American Society for Testing and Materials, Philadelphia, 1990, pp. 7-33.
5. Martin, R. H., and Murri, G. B., "Characterization of Mode I and Mode II Delamination Growth and Thresholds in AS4/PEEK Composites," *Composite Materials: Testing and Design (Ninth Volume), ASTM STP 1059*, S. P. Garbo, Ed., American Society for Testing and Materials, Philadelphia, 1990, pp. 251-270.
6. Shivakumar, K., Chen, H., and Abali, F, "A Total Fatigue Life Model for Mode I Loaded Composite Laminates," *International Journal of Fatigue*, Vol. 28, Issue 1, January 2006, pp. 33-42.
7. Johnson, W. S., and Mangalgiri, P. D., "Investigation of Fiber Bridging in Double Cantilever Beam Specimens," Journal of Composites Technology and Research, Vol. 9, No. 1, Spring 1987, pp.10-13.
8. Poursartip, A., "Characterization of Edge Delamination Growth in Laminates Under Fatigue Loading," *Toughened Composites, ASTM STP 937*, Norman J. Johnston, Ed., American Society for Testing and Materials, Philadelphia, 1987, pp. 222-241.
9. Giannis, S., Hansen, K., and Martin, R. H., "Accounting for the R-curve Effects on the Mode I Fatigue Delamination Growth Characterisation of Unidirectional Composites," *Proceedings of the American Society for Composites*, Twenty-fifth Technical Conference, Dayton, Ohio, September 20-22, 2010.
10. Murri, G. B., "Effect of Data Reduction and Fiber-Bridging on Mode I Delamination Characterization of Unidirectional Composites," *Proceedings of the American Society for Composites*, 26th ASC Annual Technical Conference/2nd Joint US-Canada Conference on Composites, Montreal, Quebec, Canada, September 26-28, 2011.
11. O'Brien, T. K., Johnston, W. M., and Toland, G. J., "Mode II Interlaminar Fracture Toughness and Fatigue Characterization of a Graphite Epoxy Composite Material," NASA TM-2010-216838, August 2010.
12. "ASTM D 5229/D 5229 M-92, Standard Test Method for Moisture Absorption Properties and Equilibrium Conditioning of Polymer Matrix Composite Materials," in *Annual Book of ASTM Standards*, Vol. 15.03, American Society for Testing and Materials, 2008.
13. Kaleidagraph, V4.1, Synergy Software, 2009.
14. "ASTM E 647-00, Standard Test Method for Measurement of Fatigue Crack Growth Rates," in *Annual Book of ASTM Standards*, Vol. 03.01, American Society for Testing and Materials, 2000.